

# Investigating the heterodimerization process among receptors by Monte Carlo cellular automaton simulation

A. Wisitsorasak, W. Triampo, D. Triampo, C. Modchang, and Y. Lenbury

**Abstract**—It has become well known that simulation can be used to investigate complex biomedical systems in situations where traditional methodologies are difficult or too costly to be used. In this paper, Monte Carlo cellular automaton simulation is employed to study heterodimerization of receptor proteins. A computer program, based on a simple random walk of receptor molecules over a fixed lattice, has been written to simulate the diffusion and association of receptors over a two-dimensional membrane. The interaction and dynamics of these particles is in the form of the lattice Hamiltonian. The formation of two-dimensional clusters of receptors in a defined area of surface membrane is investigated. In particular, we measure the number of dimers throughout the dynamics and try to define the power law that governs the process.

**Keywords**—Monte Carlo simulation, heterodimerization, membrane receptors, signal transduction.

## I. INTRODUCTION

In general, cells may communicate with each other via direct contact, over short distances, or over large distances, and they may require electrical signal, inorganic or organic substances to be messengers in their communications. Some signaling molecules such as neurotransmitters, cytokines, growth factors, although all of which are called receptor ligands, are unable to permeate the hydrophobic cell membrane. Cells receive such information from an external environment through a class of proteins known as receptors which are located on the surface membrane. To initiate intracellular signals, binding of ligands to receptors is needed [1].

This work was supported in part by the National Center for Genetic Engineering and Biotechnology.

A. Wisitsorasak is with R&D Group of Biological and Environmental Physics, Department of Physics, Faculty of Science, Mahidol University, THAILAND.

W. Triampo is with R&D Group of Biological and Environmental Physics, Department of Physics, Faculty of Science, Mahidol University, Center of Excellence for Vector and Vector-Borne Diseases, Mahidol University and Thailand Center of Excellence in Physics, THAILAND.

D. Triampo is with Center of Excellence for Vector and Vector-Borne Diseases, Mahidol University, THAILAND.

C. Modchang is with the Department of Physics, Faculty of Science, Mahidol University, THAILAND.

Y. Lenbury is with the Department of Mathematics, Faculty of Science, Mahidol University, THAILAND, Centre of Excellence in Mathematics, CHE, THAILAND (corresponding author; phone: 662-201-5448; fax: 662-201-5448; e-mail: scylb@mahidol.ac.th).

Many types of receptors such as GABA, neurotransmitter gamma-aminobutyric acid receptors, and Dopamine receptors, are activated by ligand binding individually, but some of them are activated after ligand-induced dimerization or oligomerization [2-3]. Moreover, the investigations of intracellular signal transduction pathways have revealed that the activities of several components in these pathways are also regulated by dimerization.

There are several examples in which activation of receptors are invoked after ligand-induced dimerization. The EFG receptor was the first protein-tyrosine kinase receptor to be shown to dimerize after ligand binding. The receptor for platelet-derived growth factor (PDGF), PDGF is classified as a receptor tyrosine kinase (RTK), which is the other type of cell surface receptors dimerized upon activation by PDGF. The other examples might be seen in a good review paper by Heldin [3].

The essential roles of ligand binding are different in different systems. In the case of stem cell factor (SCF) receptors, the bridging between two receptors, involving epitopes located outside the ligand-binding domains, are important for stabilization of receptor dimers. The ligand binding may work closely with related ligands and provide docking sites for downstream signal transduction molecules in heterodimeric complexes between ErbB2 and ErbB3 or ErbB4 [4]. In insulin-like growth factor 1 (IGF-1) receptor family, ligand binding does not induce receptor dimerization, but presumably causes a conformational alteration in the preformed dimeric receptor, which leads to receptor activation. These evidences can be found in the review of Heldin [3].

The human Tumor-Necrosis-Factor-Receptor-Type 1, TNFR1, which was demonstrated to be activated specifically by agonist or antibodies and to initiate a signal for cellular cytotoxicity, especially cell death, is another example of ligand-induced clustering of receptors [5-6]. This kind of receptors also plays a significant role in well known mechanism of apoptosis, or programmed cell death. In the signal transduction pathway (STP), forming oligomers of adapter proteins is an important process [7]. It is known that TNFR1 will not associate itself unless it is activated by TNF because the intracellular inhibitor, the silencer of death domain (SODD), which binds with TNFR1, will prevent its clustering [5, 8]. In addition, some molecules which block the clustering

process are binding with receptor molecules at extracellular domain [9-10]. When TNF binds TNFR1 together, any two receptors can move closer [2]. The clustering of receptors makes SODD, which is bound to a receptor in the intracellular domain, become loose from the receptor [8]. Therefore, a death receptor can bind with an adapter protein which will attach itself to a receptor molecule. The stable clustering of receptors as well as successful downstream signal responses can thus occur.

Because of the great significance of receptor dimerization, many different computational studies have been undertaken to elucidate various mechanisms and intermediate processes that can, in principle, give rise to such non-uniform receptor distribution or predict a success of downstream signaling [11]. We could categorize these computational simulation techniques in two main groups: a deterministic approach and a stochastic approach. Well known techniques such as molecular dynamics calculations, reaction-diffusion equations, numerical integration of differential equations, and master equations can be classified as deterministic. These calculations reveal information on the variables in those equations. In the same situation, however, one may want to learn about spatial characteristics of molecules interaction, and the structure of products, in which case the stochastic approach offers a better tool. The stochastic method, especially the Monte Carlo simulation, can even deal with complex systems, and examples of its applications may be found in [12-14].

Receptor clustering due to an interaction between nearest-neighbor receptors appears to be a cooperative process in a statistical mechanics point of view [2]. Recently, based on the thermodynamics model for receptor clustering, the lattice Hamiltonian of receptor dynamics was proposed by Gua and Levine in [2] and Fricke and Thomas in [15]. Their ideas can be a prototype model to simulate the dimerization process among receptors induced by ligand binding. We believe that the dimerization process of receptors induced by ligand binding is similar to a process described by an aggregation limited diffusion [16] plus the Ising model [17] in which the reaction of each particle is governed by a lattice gas Hamiltonian. Moreover, the scaling law which is a good theory to describe a diffusion process should still be applicable throughout the dimerization of receptors.

In order to examine these hypotheses further, we have written a computer program that simulates the diffusion and association of receptors over a two-dimensional membrane. The program is based on a simple random walk of receptor molecules over a fixed lattice. The interaction and dynamics of these particles is in the form of the lattice Hamiltonian which is proposed by Guo and Levine [2]. A Metropolis algorithm [18] is used to determine which configurations are lower in free energy and therefore favored. We use this program to examine the formation of two-dimensional clusters in a defined area of surface membrane containing receptor molecules of different types (unliganded receptors and liganded receptors). In particular, we measure the number of dimers throughout the

dynamics and try to define the power law that governs the process. Moreover, we investigate the outcomes of two initial configurations: random and rectangular-like distribution of receptors. Finally we interpret our results with biological application.

## II. MODEL OF DIMERIZATION PROCESS

To simplify the model for the dimerization process, we have made several assumptions. Our first step toward the ultimate goal is to provide a system of Hamiltonian that can be easily simulated and possesses the common characteristics of all dimerization processes of receptors induced by ligand binding.

This work is based on a thermodynamics model of receptors which was proposed by Guo and Levine in 1999 [2]. According to this work, the dimerization of receptors is the result of ligand binding. After binding of a ligand to an unliganded receptor, a free receptor, the state of the receptor is changed to that with a lower energy level, and it is able to be induced to form a heterodimer with other unliganded receptors. Therefore, the total number of all species of interest in our simulation is three: a liganded receptor, an unliganded receptor, and a free space.

We focus our attention on the heterodimerization process only (schematically presented in Fig. 1.). For the sake of simplicity, each receptor will be affected by the nearest neighbor receptors, called a short range interaction. Here, a clustering of receptors can be explained by means of a simple lattice Hamiltonian:

$$H = H_0 + H_I \quad (1)$$

where  $H_0$  is the potential energy of the receptor in each lattice site, and  $H_I$  is the interaction Hamiltonian between two receptors.

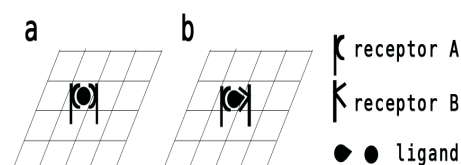


Fig. 1. Schematic representation of different forms of dimeric complexes of typical receptors after ligand binding. (a) a homodimeric complex; (b) a heterodimeric complex of two receptor subunits.

A collection of receptors is assigned to each lattice site,  $(i, j)$ , which has either one or zero receptor molecules. We denote the number of molecules in each site by  $n_i = 0$  or 1. If a lattice site  $(i, j)$  is not occupied by any receptor, we identify this situation with  $n_i = 0$ . On the contrary,  $n_i = 1$  represents an existence of a receptor at that lattice site. The lattice was occupied by two species of receptors,  $t$ ,  $t \in \{L, U\}$  where  $L$  denotes a liganded receptor and  $U$  denotes an unliganded receptor. In our case study, we assume that a ligand will only bind with a surface receptor, then called a liganded

receptor. We let the chemical potential of the ligand be  $\mu_L$  and that of the receptor be  $\mu_R$ , while  $-g_L$  is the binding energy between the ligand and the receptor. Their chemical potential contributes to the effective Hamiltonian of the system:

$$H_0(n, \tau) = -\sum_i \mu(t_i) n_i \quad (2)$$

where  $\mu(U) = \mu_R$  and  $\mu(L) = \mu_R + \mu_L + g_L$ . The summation is over all lattice sites.

Besides the chemical potential affecting the Hamiltonian, the dimerization between receptors also changes the Hamiltonian. One might write an interaction Hamiltonian in the form

$$H_I = -\sum_{\langle ij \rangle} J_{ij} a(t_i, t_j) n_i n_j \quad (3)$$

We further assume a short range interaction. Here, a nearest neighbor condition is to set  $J_{ij} = 1$  only when  $\langle i, j \rangle$  is the nearest neighbor site and  $J_{ij} = 0$  otherwise.

The function  $a(t_i, t_j)$  represents how each receptor interacts to other receptors or how much energy is required for dimerization. It is clear that this function should depend on the state of a receptor. For example  $a(U, U)$  is the energy between an unliganded receptor and an unliganded receptor,  $a(U, L) = a(L, U)$  is energy between an unliganded receptor and a liganded receptor, and  $a(L, L)$  represents the energy between a liganded receptor and a liganded receptor.

The functions  $a(U, L)$  and  $a(L, U)$  can be viewed as bond energy between these two receptors. In this simple model of dimerization, we are particularly interested in dimerization between different types of receptors. Moreover, the dimer arises via weak interaction (one or two hydrogen bonds). We will set the effective bond strength  $a(U, L)$  in the order of  $g_E = 3k_B T$  [15].

In the ligand inducing dimerization, we assume that the dimerization between similar types of receptors will rarely be formed. For the sake of simplicity, we set  $a(U, U) \approx a(L, L) \approx -g_E$ . An example of these receptors is rhodopsin which prefers to form a dimer only in some arrangements [19]. In eq. (3), we can rewrite the interaction Hamiltonian as

$$H_I = -\sum_{\langle ij \rangle} J_{ij} g_E n_i n_j \tau_i^T \begin{bmatrix} -1 & 1 \\ 1 & -1 \end{bmatrix} \tau_j \quad (4)$$

where the summation is over all lattice sites. We further define the states of receptors:

$$\tau = \begin{bmatrix} 1 \\ 0 \end{bmatrix} \text{ for } t_i = L \text{ and } \tau = \begin{bmatrix} 0 \\ 1 \end{bmatrix} \text{ for } t_i = U$$

The full form of our Hamiltonian can be written

$$\text{as } H(n, \tau) = -\sum_i n_i [\mu(1) \quad \mu(2)] \tau_i - \sum_{\langle ij \rangle} J_{ij} g_E n_i n_j \tau_i^T \begin{bmatrix} -1 & 1 \\ 1 & -1 \end{bmatrix} \tau_j \quad (5)$$

### III. MONTE CARLO SIMULATION

Cell membranes were modeled using a square lattice of  $n$  sites with periodic boundary condition, used to reduce the finite size effect. In general, cell membrane contains many kinds of particles which may move around the membrane. At the equilibrium state, any part of the membrane should have a constant flux of particles. Therefore, the periodic boundary condition is appropriate for this system. Each site on the lattice represents a possible receptor location, and each receptor's size is one lattice site. No two molecules are allowed to occupy the same lattice site. To illustrate a simple statistical model of receptor dimerization, we performed Monte Carlo simulations with the conventional Metropolis algorithm [18]. For the sake of simplicity, the number of receptors was assumed to be conserved throughout the time evolution.

Receptors were initially distributed according to a given distribution function (random distribution or rectangular distribution), but became associated as their independent random movements brought them into contact. At each time step of the algorithm,  $n$  randomly chosen sites in the lattice were selected for possible update. If the selected site,  $s_i$ , contained a receptor, then an attempt was made to randomly bring the receptor to a new nearest neighbor site,  $s_j$ . In accordance with the Metropolis Monte Carlo algorithm [18], the move is automatically accepted if it results in a decreased energy for the system, and is accepted with a probability of

$$P = \min[1, e^{-\beta \Delta H}] \quad (6)$$

where

$$\beta \equiv \frac{1}{k_B T},$$

$k_B$  is the Boltzmann constant, and  $T$  is the absolute temperature. If the target site was already occupied, then no move was made. The difference of the Hamiltonian could be calculated as described in the last section. It is important that the moves in the algorithm satisfy the detailed balance in the transition probabilities,

$$\frac{P_{i \rightarrow j}}{P_{j \rightarrow i}} = e^{-\beta \Delta H} \quad (7)$$

which is guaranteed by the Metropolis rule. The steady state of macroscopic properties of the Monte Carlo ensemble then corresponds to the thermodynamics equilibrium state of the system.

We might write a pseudo algorithm for this simulation as consisting of the following few steps.

- 1 Initialize each parameter
- 2 Monte Carlo step-loop.
- 3 Trial loop. In each trial, a particle will be randomly chosen to offer a chance of moving to a new position.
  - 3.1 Choose a particle randomly.
  - 3.2 Evaluate Hamiltonian  $H_i$  of the selected particle.

3.3 Offer a new position randomly which is close to the current position of the chosen receptor. The chosen receptor is allowed to move if the new position is free.

3.4 Assume that the chosen receptor moves to the new position already. Then evaluate Hamiltonian  $H_2$ .

3.5 Calculate a transition probability of the event in step 3.3 by means of the Metropolis algorithm. The transition probability is defined by

$$P = \min[1, e^{-\beta\Delta H}].$$

3.6 Pick a number from uniform random number generator. If the random number is greater than the probability  $P = \min[1, e^{-\beta\Delta H}]$ , the chosen receptor is allowed to move to the new position. If it is not greater than  $P$ , the event is rejected.

4 Repeat step 3, the trial loop, up the number of particles in the system.

5 Repeat steps 2 and 3, the Monte Carlo step-loop, until the system reaches a steady state.

Throughout our simulation, we are interested in the heterodimerization of receptors. We consider the evolution of the system as it undergoes dimerization process. We qualitatively monitor the temporal evolution of a dimering parameter (or disordering parameter),

$$A = \sum_i \sum_j \{1 - \delta(n_i, n_j)\} J_{ij} \quad (8)$$

where  $J_{ij} = 1$  only when  $i, j$  are nearest neighbors and is 0 otherwise, and the summation is done over all lattices  $i$  and  $j$ . The delta function  $\delta(n_i, n_j) = 1$  if  $n_i$  is the same as  $n_j$ , and  $\delta(n_i, n_j) = 0$  otherwise.

First, both types of receptors are located at different lattice sites with periodic boundary condition. In the simulation, a filled circle and an open circle represent a liganded receptor and an unliganded receptor, respectively. A particle will be randomly selected in each trial to offer a chance of moving to a new position.

If a chosen particle lives without other receptors in its nearest neighborhood, it moves like a free diffusion. The unliganded receptor in Fig. 2a, which is denoted by the filled circle, is offering an opportunity to move to the right. Clearly, the Hamiltonian of this particle,  $H_1$ , is equal to  $H_0$ . If it has already moved to the new lattice site (Fig. 2b), the new Hamiltonian,  $H_2$ , must be evaluated and is equal to  $H_0$ . After that, a transition probability  $P = \min[1, e^{-\beta\Delta H}]$  will be calculated. In this case, one sees that  $P = 1$  which means that the particle will definitely move to the lattice site on the right as in Fig. 2b.

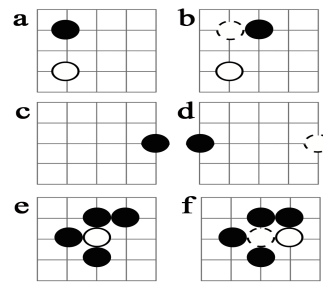


Fig. 2. Series of snapshots showing possible events which might occur in the simulation. An open circle denotes an unliganded receptor and a filled circle represents a liganded receptor.

In the same situation, a liganded receptor, a filled circle, appears at a right most lattice site (Fig. 2c) and is moving to the right. Because of the periodic boundary condition, that particle will move to the leftmost lattice site within the same row (Fig. 2d). We note that the periodic boundary condition is used to reduce a finite size effect, applicable when the spatial scale of the membrane is very large compared to those of the receptors.

Fig. 2e shows an unliganded receptor, an open circle, surrounded by three liganded receptors, filled circles. This simulation considers only the short range interaction; therefore, the interaction between the farthest filled circle particle and the open circle particle is omitted. The Hamiltonian of the open circle particle is equal to  $H_1 = H_0 + 3g_E$ . If it is moving to the right, Fig. 2f, the new Hamiltonian will be equal to  $H_2 = H_0 + g_E$ . The lower energy renders the particle with the tendency to move to the right with the transition probability  $P = \min[1, e^{-2g_E/\beta}]$ .

#### IV. RESULTS AND DISCUSSION

Throughout, a number of simple Monte Carlo simulations were first conducted in order to verify that thermodynamically expected behavior is reproduced in a simple system and two-dimensional aggregates are produced. All simulations were performed with two types of receptors, liganded receptors (L) and unliganded receptors (U), on a square lattice with the periodic boundary condition.

Fig. 3. shows the result of a typical simulation. Both receptors were initially distributed at random positions (Fig. 3a.), but became associated as their independent random movements brought them into contact. After 104 steps (Fig. 3c.), many dimers had formed.

As the simulation continued, the number of dimers or clusters seemed to slightly fluctuate. We assessed the extent of dimerization by counting the number of broken bonds, a term used as a dimering parameter (Fig. 4., open circles corresponding to AB-Bonds). Other measurements were also made such as the number of similar bonds, bonds between the same species (Fig. 4., filled circles), the mean cluster size, and the number of monomeric molecules.

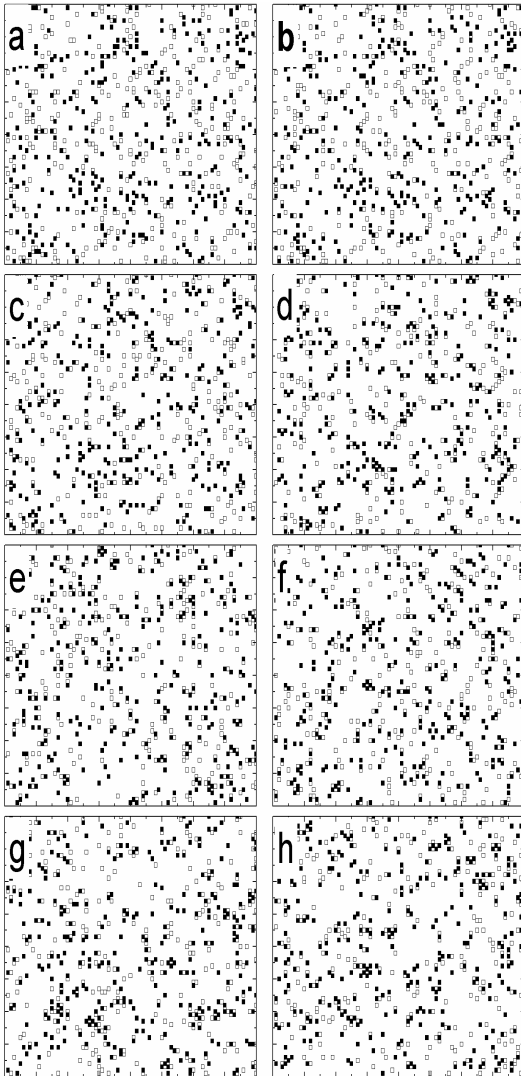


Fig. 3. Sequence of snapshots showing the dimerization process of a  $80 \times 80$  system with  $[C_L] = [C_U] = 5\%$ . The filled and opened squares represent liganded receptors and unliganded receptors, respectively, and the white region denotes the free space. The configurations were recorded at 0, 10,  $10^2$ ,  $10^3$ ,  $10^4$ ,  $10^5$ ,  $10^6$ , and  $10^7$  MCS.

This study was concerned with the kinetics, rather than the equilibrium state. From Fig. 4., we focused on the intermediate regime, but the simulation was still performed until the time step of  $10^7$  at which the system had reached the steady state. The numbers of both types of bonds are constant beyond this time step. To obtain the smooth curves and small fluctuations, the simulations under typical conditions were repeated several times. We then used these averaged results in our analysis. The straight reference line which appears in the second regime (I) has slope  $0.252 \pm 0.001$  and the saturation curve in the last regime (S) yields to the number of the broken bonds at equilibrium state which is  $252 \pm 5$ . We also found that the crossover time  $t_L$  is  $353 \pm 5$ .

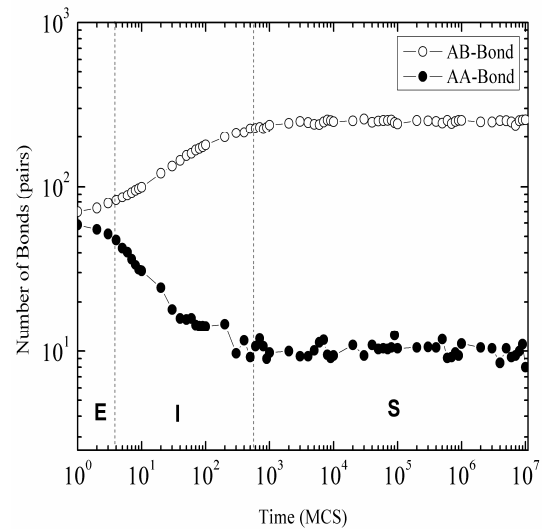


Fig. 4. Plot of the broken bond (AB-Bond) and the similar bond (AA-Bond) against Monte Carlo Step (MCS) for a  $80 \times 80$  system with concentration of liganded and unliganded receptors:  $[L] = [U] = 5\%$ . We observe the emergence of an early region (E), an intermediate region (I), and a late or saturation region (S). The line of AB-Bonds appears almost symmetrical to that of AA-Bonds.

The formation of the number of broken bonds is influenced by a large number of factors, and it is almost impossible to identify all of them. Nevertheless, we might initially guess that the number of broken bonds mainly depends on four quantities: the lattice size  $L$ , the concentration of liganded receptors  $C_L$ , the concentration of unliganded receptors  $C_U$ , and time  $\hat{t}$ . It is not unreasonable to expect that there is a basic law which determines the number of broken bonds in terms of these factors. In the fractal concepts [10], the relationship between the number of the broken bonds  $A(L, C_L, C_U; \hat{t})$  and the time step in the intermediate regime can be assumed as

$$A(L, C_L, C_U; \hat{t}) \sim \hat{t}^\beta \quad (9)$$

The exponent  $\beta$ , which we call a dimering exponent, characterizes the time-dependent dynamics of the heterodimerization process. However, the dynamics of the system does not only depend on a time step  $\hat{t}$ , but also conditional on the lattice size  $L$ .

#### 4.1 Effect of System Size on Receptor Dynamics

We performed a series of simulations in which the equilibrium state was measured for different starting parameters, especially the system size. We varied the system size by letting  $L \times L = 40 \times 40, 60 \times 60, 80 \times 80$ , and  $200 \times 200$ . Even though the system size changes, the concentrations of liganded receptors and unliganded receptors are fixed:  $[C_L] = [C_U] = 5\%$ . The other parameters and conditions are similar to those in the previous section.

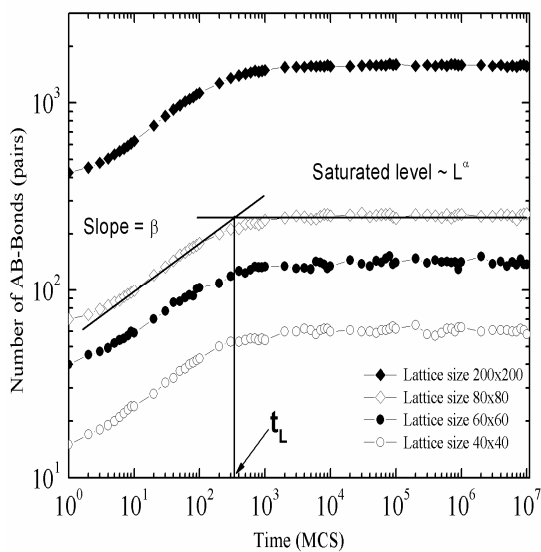


Fig. 5. Data on the number of heterodimer (AB-Bond) versus Monte Carlo Step at the lattice sizes  $40 \times 40$ ,  $60 \times 60$ ,  $80 \times 80$ , and  $200 \times 200$ .

From the plots in Fig. 5 of the number of broken bonds against Monte Carlo steps, for four sizes of the lattice, it may be seen that all curves display similar behaviors. They go through a relaxation period in the first regime (E). Then the numbers of broken bonds grow steadily. Finally they become constant in time.

When the system reaches the equilibrium state, the number of broken bonds depending on the system size could be expressed as [10]

$$A(L, C_L, C_U; t \rightarrow \infty) \sim L^\alpha \quad (10)$$

where  $\alpha$  was the disordering exponent. According to Fig. 5., the saturated exponent  $\alpha$  was found to be  $2.010 \pm 0.004$  for all the sizes considered.

The simulation results and the power law assumption in Eq. (9) and (10) can be combined into a finite-size scaling expression of the form

$$A(L, C_L, C_U; t) \sim L^\alpha f\left(\frac{t}{t_L}\right) \quad (11)$$

where  $f(x)$  is a scaling function defined by

$$f(x) \sim \begin{cases} x^\alpha & \text{for } x \ll 1, \\ \text{constant} & \text{for } x \gg 1, \end{cases}$$

To test this assumption, we plotted  $A(L, C_L, C_U; t) / L^\alpha$  against  $t / t_L$  for several values of the system size. Fig. 6 shows that, with the chosen parameter values, the data points are collected along a single curve, supporting the validity of the scaling assumption in (11).

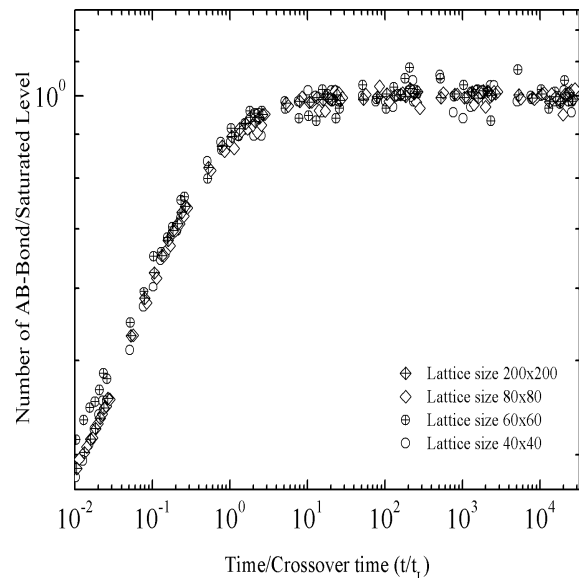


Fig. 6. The data in Fig. 5. re-plotted with  $L^\alpha f(t/t_L)$ . Here,  $\alpha = 2.0$  and  $t_L = 370$  have been used to collapse all of the data points onto a single curve.

#### 4.2. Effect of Substrate Concentration

We now turn our attention to different initial concentrations of liganded and unliganded receptors. For each case, four different lattice sizes,  $40 \times 40$ ,  $60 \times 60$ ,  $80 \times 80$ , and  $200 \times 200$ , are studied. The other parameters, such as the coupling energy, and the square lattice size, are the same as in the previous simulations. Either liganded receptors or unliganded receptors are equivalent in terms of the physical meaning. They are symmetric variable. The outcome from using the concentrations of liganded and unliganded receptors of 5% and 10%, or 10% and 5%, respectively, is the same. The two cases could have been interchangeable.

The influence of the system size and the substrate concentration on the same set of parameters is shown in Fig. 7. With the same concentrations of both types of receptors, the dimerization process gradually progress in the same way. Curves in each panel seem to differ in the y-values only. The dynamics of the system were obviously discernible if we compared the results with other panels. For fixed value of the system size while changing the number of receptors, the level of the broken bond counts might increase or decrease. The more number of receptors, the higher the curves. The dimerization process was clearly reflected in the broken bond  $A(L, t)$ . As seen in Fig. 7., one could also obviously identify three separate regions which have already been observed. It should be noted that the I and S regions emerge only in a finite system. We evaluated the exponents  $\alpha, \beta$  and the crossover time  $t_L$  and show them in Table 1.

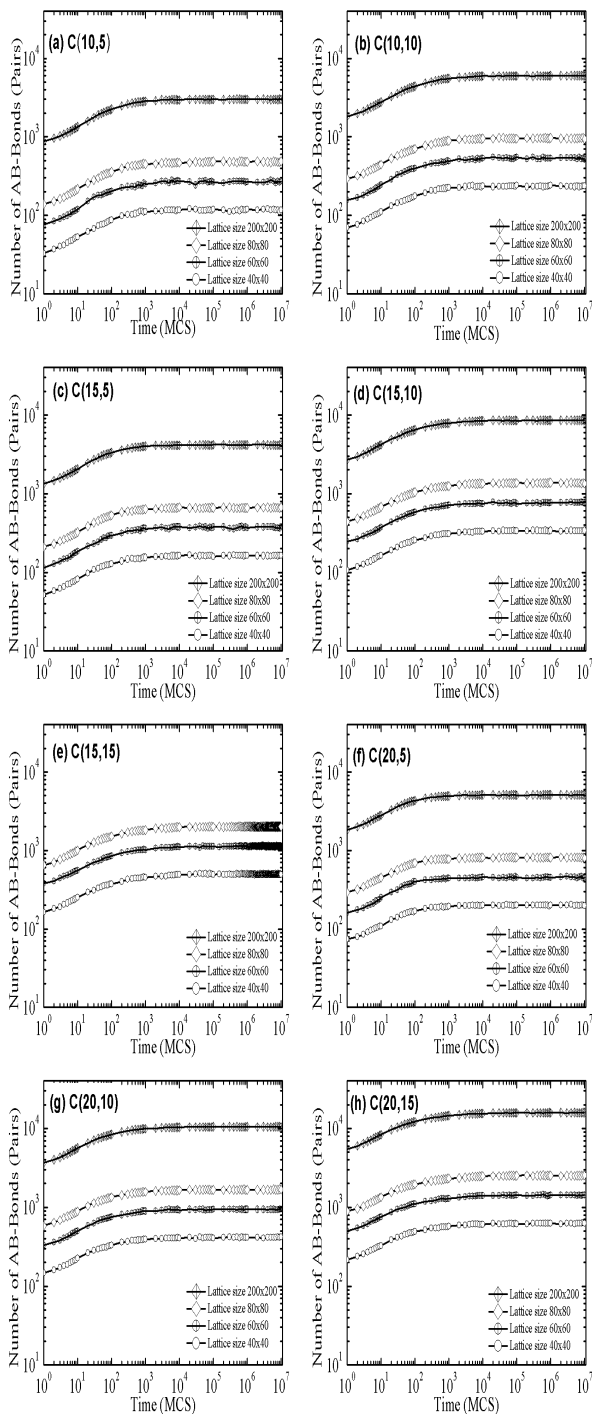


Fig. 7. Simulation in investigation of the effect of both concentration of receptors and lattice size on the receptor dynamics. In each graph, the number of the broken bonds corresponding to the same concentration of substrate was plotted against the Monte Carlo Step. We studied the eight cases of concentrations of receptors. In figure (a) to (h), the concentrations of liganded receptors and unliganded receptors are shown in the number pairs  $([C_L], [C_U])$  as (10,5), (10,10), (15,5), (15,10), (15,15), (20,5), (20,10), (20,15), (20,20), respectively.

Lattice size	Saturated no. of broken bonds	Dimering exponent ( $\beta$ )	Crossover time ( $t_L$ )
40	61.01	$0.246 \pm 0.003$	392.39
60	140.27	$0.248 \pm 0.002$	384.98
80	251.53	$0.252 \pm 0.001$	353.19
200	1581.30	$0.247 \pm 0.001$	375.96

Table 1. Parameter values from the simulation data shown in Fig. 5, giving the saturated number of the broken bonds, the saturated exponent ( $\beta$ ), and the crossover time ( $t_L$ ).

It is natural to ask whether the scaling forms found in the previous section still hold. We present the scaled plot of the number of broken bonds,

$$A(L, C_L, C_U; t) / A_{sat}(L, C_L, C_U; t)$$

against  $t/t_L$ , in Fig. 8. With the same concentration of receptors, we easily found that all graphs collapse down to a single curve which supported the scaling hypothesis. The three temporal regimes are well separated and easy to distinguish. In each intermediate regime the number of broken bonds follows different power laws. The slopes of the straight lines are shown in the Table 1. Unlike the last regions, the saturation number of the broken bonds is governed by the  $L^2$  power law which is independent of receptor concentration. One might explain that this  $L^2$  power law has been derived from the 2-dimensional space. Even though the number of each kind of receptors increases as the lattice size increases, the concentration, the ratio of number of particles to the total lattice size, was constant. Each particle in the same concentration was aware of the same characteristic length scale. Therefore, the saturation number of the broken bonds increases relatively to the increasing number of particles, according to the  $L^2$  power law. Due to the same characteristic length which each particle sees, the systems also reach the steady state at the same crossover time  $t_L$ .

Why is a scaling law still valid for the number of broken bonds in the system which has the same concentration? The key to this question is the interaction among particles in the system [20]. The interaction among particles directly defines the growth of the number of broken bonds. This interaction does not depend only on the lattice Hamiltonian, but also on how many receptors there are. However, for the systems with the same concentration, the same scaling law is still applicable.

One assumption we have used is that receptors start with a random distribution. However, the real configuration of receptors on the cell membrane does not always appear in a random fashion. One possibility is that receptor molecules might cluster themselves into different distributions (Fig. 9a). Will the dynamics of the system be the same as those observed in the previous simulations? This could be examined by starting the simulation with receptors in different kinds of distribution.

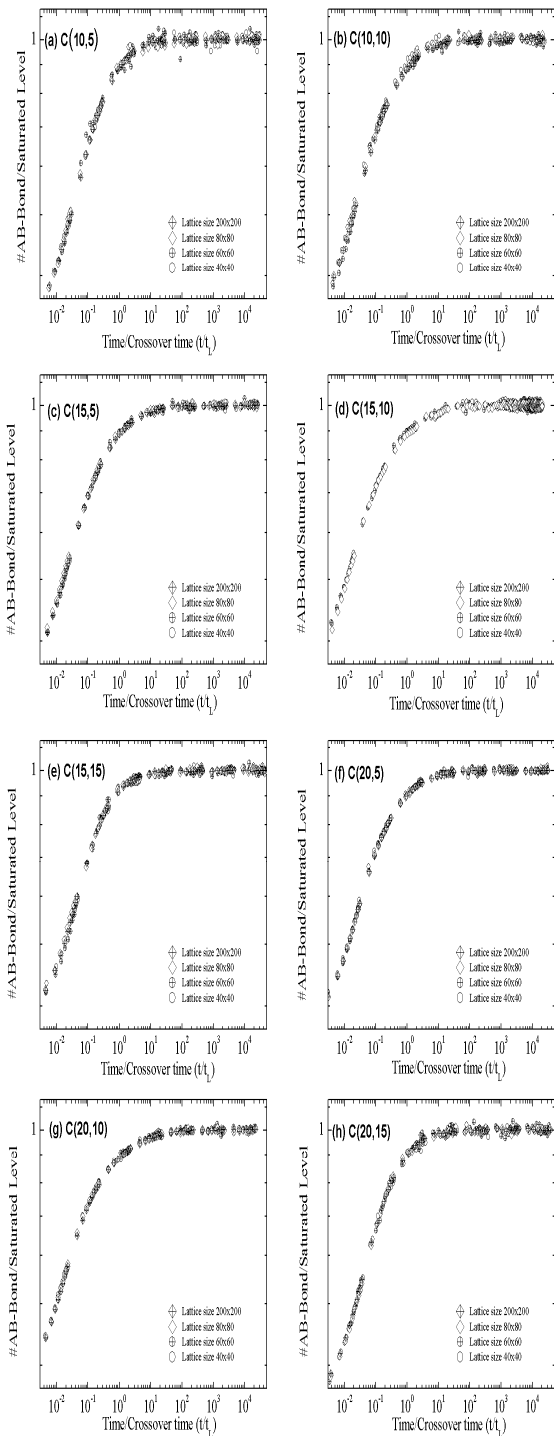


Fig. 8. The data in Fig. 7. re-plotted with  $L^\alpha f\left(\frac{t}{t_L}\right)$ . In all figures, the saturated exponent  $\alpha \sim 2.0$  and the corresponding crossover time  $t_L$  have been used to collapse all of the data onto a single, unique curve  $f(x)$ . The curves are increasing for  $x < 1$  with  $\beta \sim 0.24$ , but constant for  $x > 1$ .

4.3. Effect of Initial Configuration

In this section, we will discuss simulations starting from a rectangular arrangement of homodimers. The two species are spatially segregated (shown schematically in Fig. 9a.).

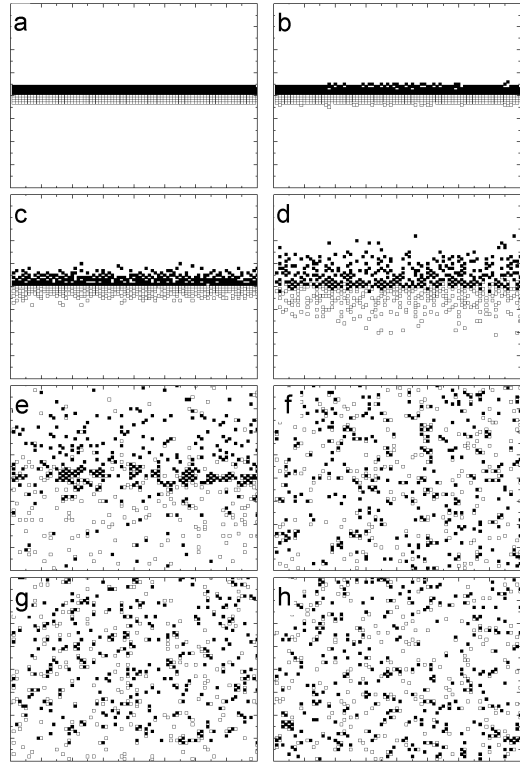


Fig. 9. The visual impressions of the dimerization process of the system starting with a rectangular island distribution. The set of parameters used is the same as that of Fig. 4. The filled squares and the open squares represent liganded receptors and unliganded receptors, respectively, and the white region denotes the free space. The configurations are recorded after 0, 10,  $10^2$ ,  $10^3$ ,  $10^4$ ,  $10^5$ ,  $10^6$ , and  $10^7$  MCS.

The receptors are initially clustered horizontally in the middle of the lattice. Each group of receptors forms a smooth interface. We call this distribution a rectangular island distribution. To examine the dynamics of the system, we performed Monte Carlo simulations of receptor dimerization with two receptor species present. Quantitatively, the visual impressions of the dimerization process of such initial configuration is seen in Fig. 9. In this case, the initial interface at  $t = 0$  is completely smooth. As time progresses, the interface begins to break up slowly as the receptors diffuse away to occupy the free space. As more particles diffuse to the opposite side, roughening of the interface begins. As time goes by, the degree of heterodimerization becomes larger and the interface fades away. Eventually, at steady state, the two receptor species appear well-mixed or become homogeneously mixed (Fig. 9h.).

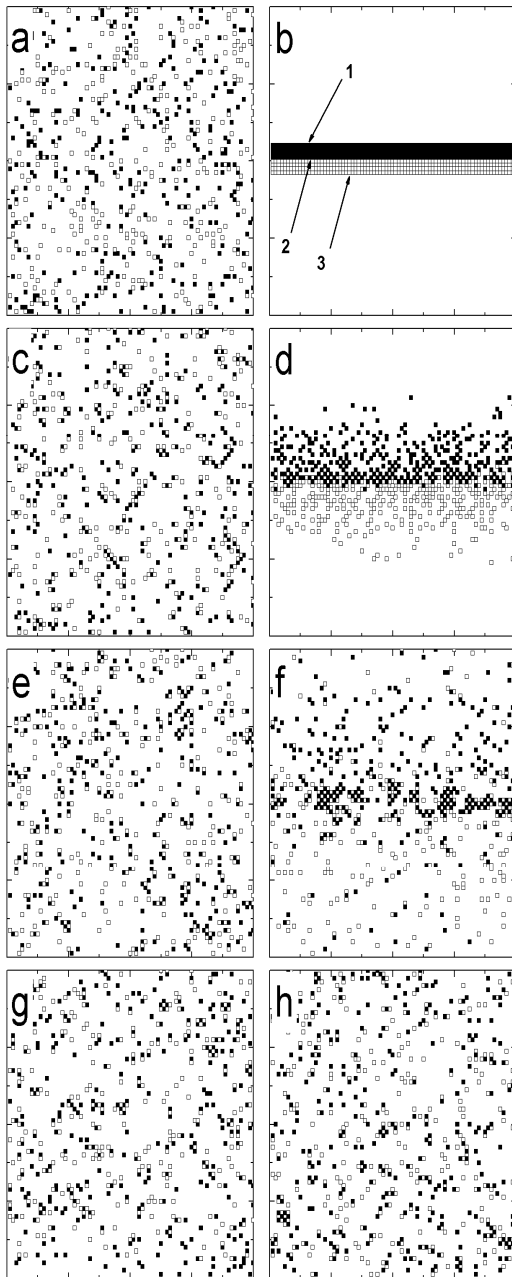


Fig. 10. Comparison of snapshots of the system starting with a random distribution (left column) and the rectangular island arrangement (right column). The figures on the left side and the right side were recorded at the same time steps for comparison. Figures (a), (c), (e), and (g) correspond to time steps of  $0, 10^3, 10^4$ , and  $10^7$ , respectively.

To compare the rectangular island arrangement with the random distribution, the sequences of snapshots of these two initial configurations are shown in Fig. 10. In both simulations,  $[C_L] = [C_U] = 5\%$ ,  $g_E = 3k_B T$ , and the lattice size =  $80 \times 80$ .

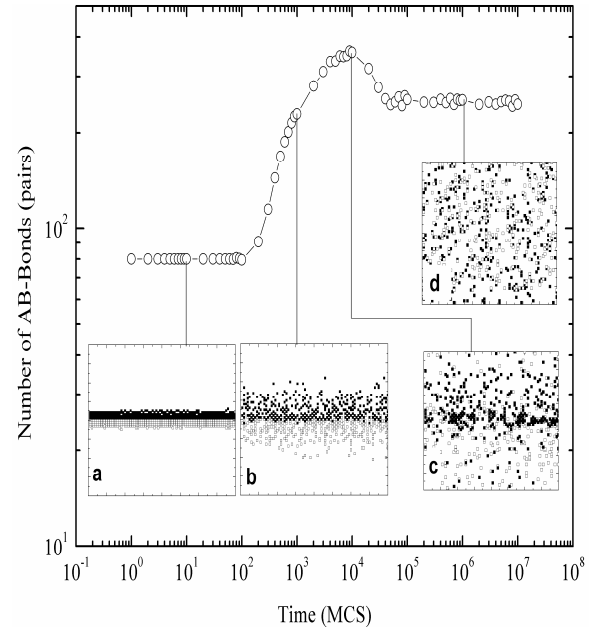


Fig. 11. The time evolution of the number of broken bonds. The system is identical to those in Fig. 7. The configurations in (a), (b), (c), and (d) are pictures taken at time steps of  $10, 10^3, 10^4$ , and  $10^6$ .

While snapshots of simulation results are illuminating, it is also useful to obtain more quantitative measures of heterodimerization by calculating the number of broken bonds from snapshots and then averaging over ten iterations. In Fig. 11, some visual impressions of the dimerization process and the number of broken bonds are presented as time evolution. From the graph, the dynamics of this system is obviously different from the system subject to an initial random distribution observed in the previous section. We divided the curve in Fig. 11, into three main regions in the same manner as in the Fig. 4: an early region (E), an intermediate region (I), and a saturation region (S). The first region (E) from the rectangular island distribution seems longer than that from the random distribution. Moreover, we even observe the shooting up peak in the intermediate region (I). These phenomena could give an intuitive understanding of the system. We can divide the interface region in Fig. 10b, into three interfaces labeled in the figure. In the early steps, Fig. 11a., the interface 2 is still unchanged as receptors at the interfaces 1 and 3 attempt to occupy the vacancy. The number of broken bonds remains constant. As the time went by, Fig. 11a, the interfaces 1 and 3 disappear while the receptors at the interface 2 still are unable to move because of their neighbors. As more particles diffuse, the receptors at the interface 2 are free to move and they are likely to aggregate in big clusters. These islands cause the highest number of the broken bonds. After that the big clusters crack into small ones, and the curve goes down. Eventually, at steady state, the system becomes completely mixed as in the system that starts from a the random distribution.

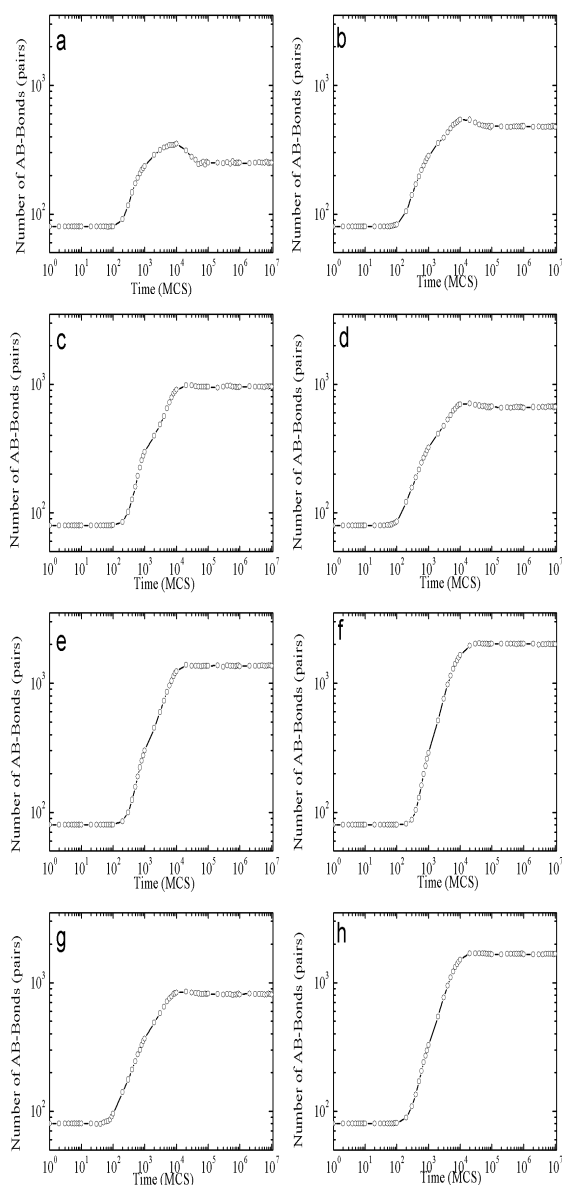


Fig. 12. Time evolution of the number of broken bonds. The system was initiated with the rectangular island arrangement and the lattice size was  $80 \times 80$ . The dynamics of receptors changed differently when the selected concentrations of liganded receptors and unliganded receptors are (in pairs of  $([C_L], [C_U])$ ) (5,5), (10,5), (10,10), (15,5), (15,10), (15,15), (20,5), and (20,10), respectively.

We now turn to our simulation that investigates the effect of substrate concentrations on the dynamics of the system with the rectangular island distribution. We counted the number of the broken bonds at each time step and plotted the results in Fig. 12. Comparing Fig. 12. to Fig. 7., they both share the same saturation level in the last region. In contrast to the system with the random initial configuration, here the early regime (E) takes longer time because the mobility of particles is limited by the initial configuration. The particles in the random distribution have more freedom than those in the rectangular island distribution. In addition, their initial

distribution and the concentration of substrates directly affect the dynamics in the intermediate region (I). According to Fig. 12., we can observe the shooting up peak in the low concentration cases. However this peak is not observed in the higher concentration.

A reasonable explanation is that the big clusters at the interface 2 (Fig. 11c.) would be dominant only in the low number of receptors. When the number of receptors increases, that peak is lost due to the number of heterodimers in other regions.

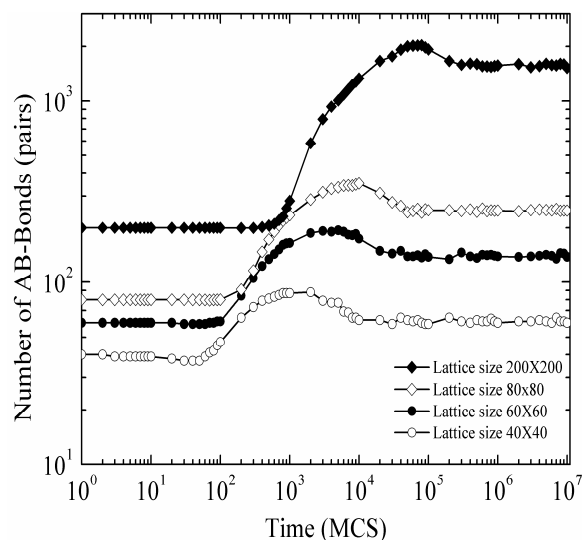


Fig. 13. The change in the number of broken bonds for the systems starting with a rectangular island distribution. Simulations were run for various lattice sizes:  $40 \times 40$ ,  $60 \times 60$ ,  $80 \times 80$ , and  $200 \times 200$ , while the concentration was kept at 5%.

Finally, we varied the system size with the rectangular island arrangement at constant concentration. Fig. 13. presents the time evolution of the number of broken bonds for different system sizes,  $40 \times 40$ ,  $60 \times 60$ ,  $80 \times 80$ , and  $200 \times 200$ . Here, the concentrations of the liganded receptors and the unliganded receptors are both 5%. Clearly, the shift of the crossover time is observed. The larger the system size, the higher the crossover time becomes.

Apparently, the system in which the receptors are initially arranged in the rectangular distribution configuration is effected by the lattice size. In comparison to the system of receptors with the initially random distribution, the crossover time is shifted toward the right of the time axis. This is because the system of receptors with the initial rectangular distribution needs more time to rearrange itself to the same equilibrium as the system with the initial random distribution.

#### ACKNOWLEDGMENT

Appreciation is extended toward the National Center for Genetic Engineering and Biotechnology.

## REFERENCES

- [1] N. A. Campbell, J. B. Reece, *Biology*, Benjamin Cummings, 2004.
- [2] C. Guo, H. Levine, A thermodynamic model for receptor clustering, *Biophys J*, Vol. 77, 1999, pp. 2358-65.
- [3] C.-H. Heldin, "Dimerization of cell surface receptors in signal transduction," *Cell*, Vol. 80, 1995, pp. 213-223.
- [4] E. Peles, R. Ben-Levy, E. Tzahar, N. Liu, D. Wen, Y. Yarden, "Cell-type specific interaction of Neu differentiation factor (NDF/hergulin) with Neu/HER-2 suggests complex ligand-receptor relationships," *EMBO Journal*, Vol. 12, 1993, pp. 961-971.
- [5] L. A. Tartaglia, D. V. Goeddel, "Tumor necrosis factor receptor signaling. A dominant negative mutation suppresses the activation of the 55-kDa tumor necrosis factor receptor," *Journal of Biological Chemistry*, Vol. 267, 1992, pp. 4304-4307.
- [6] L. L. Kiessling, J. E. Gestwicki, L. E. Strong, "Synthetic multivalent ligands in the exploration of cell-surface interactions," *Curr Opin Chem Biol*, Vol. 4, 2000, pp. 696-703.
- [7] A. Ashkenazi, V. M. Dixit, "Death receptors: signaling and modulation. Science," Vol. 281, 1998, pp. 1305-8.
- [8] Y. Jiang, J. D. Woronicz, W. Liu, D. V. Goeddel, "Prevention of constitutive TNF receptor 1 signaling by silencer of death domains," *Science*, Vol. 283, 1999, pp. 543-6.
- [9] M. P. Boldin, I. L. Mett, E. E. Varfolomeev, I. Chumakov, Y. Shemer-Avni, J. H. Camonis, D. Wallach, "Self-association of the "death domains" of the p55 tumor necrosis factor (TNF) receptor and Fas/APO1 prompts signaling for TNF and Fas/APO1 effects," *J Biol Chem*, Vol. 270, 1995, pp. 387-91.
- [10] V. Vandevoorde, G. Haegeman, W. Fiers, "Induced expression of trimerized intracellular domains of the human tumor necrosis factor (TNF) p55 receptor elicits TNF effects," *J Cell Biol*, Vol. 137, 1997, pp. 1627-38.
- [11] J. Goldman, S. Andrews, D. Bray, "Size and composition of membrane protein clusters predicted by Monte Carlo analysis," *European Biophysics Journal*, Vol. 33, 2004, pp. 506-512.
- [12] V. M. Ivanov, M. L. Korenevsky, "Sequential Monte Carlo and adaptive numerical simulation," *WSEAS Trans. Syst.* Vol. 3 (8), 2004, pp. 2694-2698.
- [13] A. J. Vand, S. Khanmohammadi, F. Shabani Nia, "Hybrid modeling and simulation of robotic manufacturing system using time Petri nets," *WSEAS Trans. Syst.* Vol. 4 (5), 2005, pp. 513-520.
- [14] G. Tont, M. Iliescu, D. G. Tont, "A methodology of availability assessment for complex manufacturing systems," *WSEAS Trans. Syst.* Vol. 7 (6), 2008, pp. 822-832.
- [15] G. M. Fricke, J. L. Thomas, "Receptor aggregation by intermembrane inter-actions: a Monte Carlo study," *Biophys Chem*, Vol. 119, 2006, pp. 205-11.
- [16] T. A. Witten, L. M. Sander, "Diffusion-limited aggregation," *Physical Review B*, Vol. 27, 1983, pp. 5686.
- [17] K. Binder, "Applications of Monte Carlo methods to statistical physics," *Reports on Progress in Physics*, Vol. 60, 1997, pp. 487.
- [18] M. Nicholas, A. Rosenbluth, M. Rosenbluth, A. Teller, E. Teller, "Equation of State Calculations by Fast Computing Machines," *Journal of Chemical Physics*, Vol. 21, 1953, pp. 1087-1092.
- [19] B. Jastrzebska, T. Maeda, L. Zhu, D. Fotiadis, S. Filipek, A. Engel, R. E. Stenkamp, K. Palczewski, "Functional characterization of rhodopsin monomers and dimers in detergents," *J Biol Chem* 279, 2004, pp.54663-75.
- [20] A.-L. Barabási, H. E. Stanley, *Fractal Concepts in Surface Growth*, Cambridge University Press, (1995).